Desalination and Water Treatment
www.deswater.com
doi: 10.1080/19443994.2015.1027278

57 (2016) 8967–8980
April

Taylor & Francis
Taylor & Francis Group

Application of bifunctional *Mangifera indica* L.-loaded *Saccharomyces cerevisiae* as efficacious biosorbent for bivalent cobalt and nickel cations from different wastewaters: equilibrium and kinetic studies

Amr A. Yakout[a,b,*], Medhat A. Shaker[a,c], Hassan M. Albishri[d]

[a]*Faculty of Science, Chemistry Department, University of Jeddah, Jeddah, Saudi Arabia, Tel. +201001609201; email: Amryakout157@gmail.com (A.A. Yakout), Tel. +966553471259; email: drmashaker@yahoo.com (M.A. Shaker)*
[b]*Faculty of Science, Chemistry Department, Alexandria University, Alexandria, Egypt*
[c]*Faculty of Science, Chemistry Department, Damanhour University, Damanhour, Egypt*
[d]*Faculty of Science, Chemistry Department, King Abdulaziz University, Jeddah, Saudi Arabia, Tel. +9666545550373; email: hmalbeshri@kau.edu.sa*

Received 15 October 2014; Accepted 1 March 2015

ABSTRACT

Baker's yeast (*Saccharomyces cerevisiae*) was immobilized on mango (*Mangifera indica* L.) leaves to prepare a novel, low cost, and eco-friendly biosorbent Mi-yeast. The fabricated biosorbent was characterized by FTIR and SEM and applied to remove Co(II) and Ni(II) ions from aqueous solutions via batch mode technique. The biosorption equilibria were established in 30 min and the experimental data were applied to Freundlich, Langmuir, and Dubinin–Radushkevich isotherm models. The maximum biosorption capacities were found to be 526 mg g^{-1} for Co(II) at pH 6 and 250 mg g^{-1} Ni(II) at pH 7. Among four kinetic models, the experimental data were best described by the second-order expression. Different foreign ions were found to have a negligible interfering effect on the biosorption capacities. Mi-yeast could be regenerated using 0.2 M HCl during repeated biosorption–desorption cycles with 4–7% loss in metal efficiency after five cycles. The potential applications of Mi-yeast for selective removal of Co(II) and Ni(II) from different real wastewater samples of different matrices were also applied using a micro-column technique.

Keywords: Biosorption; *Mangifera indica*; Co(II); Ni(II); Yeast; Wastewater

1. Introduction

Heavy metals can be classified into four major groups as essential, such as Cu, Zn, Co, Cr, Mn, and Fe which are micronutrients and toxic when taken in excess, non-essential such as Ba, Li, and Zr, less toxic such as Sn and Al, and highly toxic such as Hg, Pb, and Cd [1]. The great expansions in anthropogenic activity and industrial technologies have generated large quantities of aqueous effluents containing heavy metals with great toxicity beyond the permissible limits due to their non-biodegradability and bioaccumulation that pose a significant threat to the environment and public health [2,3]. Heavy metal toxicity may result in a number of health problems including damaged or reduced mental and central nervous function, lower energy levels, and damage to blood composition, lungs, kidneys, liver, and other vital organs. These possible

*Corresponding author.

detrimental impacts of heavy metals on the human, biological organisms, and ecological systems make it necessary to apply ever-increasing standards of pollutant detection and treatment and to search for efficient extraction processes for toxic metals from wastewaters [2–5]. Accordingly, many countries set very strict legislations to limit the concentration of heavy metals in aquatic life. The maximum permissible concentration limits for cobalt and nickel given by WHO and United States Environmental Protection Agency were 100 and 70 μg L^{-1}, respectively. Several chemical and physicochemical technologies for removing heavy metals from wastewater such as chemical precipitation, hyperfiltration, ion exchange, electrochemical treatment, membrane technologies, floatation, adsorption, evaporation, reverse osmosis, and photocatalysis could be applied to remove heavy metals from polluted waters [6–16]. However, these techniques might either have low removal efficiencies or high expenses and secondary pollutions, especially at low concentrations of metal ions. Biosorption seems a promising and often used alternative method to remove contaminants from domestic and industrial effluents with minimal energy, high efficiency, low cost, possibility of regeneration of the biosorbent, minimization of secondary pollution, and minimal impact on the environment. Biosorbents contain various functional groups as carboxylic (galacturonic acids in pectin), phosphate, sulfate, amino, amide, and hydroxyl (in cellulose) that are known to strongly bind metal cations in aqueous solution. Typical biosorbents can be derived from three main sources, the first source is the non-living biomass such as plant materials, bark, lignin, shrimp, krill, squid, crab shell, etc.; the second source is the algal biomass, and the third one is the microbial biomass, e.g. bacteria, fungi, and yeast. Natural biosorbents from agricultural byproducts that are environmentally safe and easily available in large quantities could be potentially low-cost adsorbents, as they represent unused resources. Actually, no exclusive investigation has been carried out on the ability of mango (*Mangifera indica*) leaves as biosorbent for the extraction, treatment, and removal of heavy metal ions from wastewater samples. Instead, mango bark powder was investigated in some batch equilibrium biosorption systems. Yeast (*Saccharomyces cerevisiae*) was successfully applied in selective biosorption for a number of metals from different matrices. To improve the biosorption capacity of biosorbents, various types of modifying agents have been applied [17–19]. Immobilization of yeast on another biosorbent surface was found to improve its interaction properties with metal ions [17–19]. Searching for low-cost, non-conventional, abundant, economically viable, and environmentally safe biomaterials that can interact effectively with heavy metals to ppb levels is the main focus of our research works [20–30]. The objective of this work was to investigate the potential and the efficiency *of* yeast immobilized-*Mangifera* leaves powder (Mi-yeast) for the biosorptive extraction of Co(II) and Ni(II) from aqueous solutions and comparing its metal capacity with the native leaves (Mi). The effects of medium pH, contact time, initial adsorbate concentration and sorbent dose on the biosorption capacity, and removal efficiency were investigated by batch and micro-column techniques. Langmuir, Freundlich, and Dubinin–Radushkevich adsorption models were applied to the experimental adsorption data. Different kinetics models were tested to determine the rate expression of biosorption processes. In addition, the potential applications of Mi and Mi-yeast biosorbents for effective heavy metal ions removal from real contaminated samples have been accomplished to test the environmental impact and significant role of those biosorbents in controlling the removal, mobility, and bioavailability of metal ions in the environment. The reusability of the batch and micro-column studies was performed by carrying out different cycles of biosorption and desorption.

2. Materials and methods

2.1. Chemicals and reagents

All chemicals (Aldrich Chemical Company) used in this work were of analytical reagent grade. Baker's yeast (*S. cerevisiae*) was purchased from local commercial company. Anhydrous cobalt(II) chloride and nickel(II) sulfate salts were dissolved in double distilled water to prepare stock solutions (0.1 M) for each metal. One liter buffer solutions (pH 1.0–7.0) were prepared by mixing appropriate volumes of HCl (1.0 M) and $CH_3COONa{\cdot}3H_2O$ (1.0 M) solutions in double distilled water. The pH-value of each buffer solution was adjusted using Orion pH-meter.

2.2. Preparation of [Mi] and [Mi-yeast] biosorbents

Mango leaves, Mi were collected from trees grown in an organic fertilized soil. The leaves were washed four times thoroughly with double distilled water and air-dried. The dried leaves were ground to fine solid powder and sieved to 80 μm particle sizes. The yeast biomass was dried in a hot air oven at 60°C for 2 h. The immobilization of yeast was carried out by mixing 100 g of dry Mi powder, 50 g of powdered baker's yeast, and 15 ml double distilled water then dried at 60°C for complete dryness. The composite matrix was further well mixed with 15 ml of double distilled water

and then left for complete dryness. This procedure (mixing and drying) was repeated five times to obtain a homogenous biopolymer-assisted composite powder, Mi-yeast as a novel biosorbent of yellow–brown color. Finally, the wet mixture was dried for 24 h.

2.3. Instrumentations

The scanning electron microscope, SEM (JEOL-JSM-5300) was used to study the surface morphology and characterization of biosorbents. FTIR spectra were performed for characterizing the investigated the biosorbents using Perkin–Elmer (FTIR system-BX 0.8009) in the range 350–4,000 cm^{-1}. The Shimadzu atomic absorption spectrophotometer (AAS) AA-6800 was used together with the auto sampler Shimadzu ASC-6100 used to determine Co(II) and Ni(II) concentrations at the proper wavelengths. An Orion pH meter model 420A was used to measure the pH of the sorption reaction mixtures.

2.4. Biosorption studies

All batch biosorption experiments were performed as single component batch systems in triplicate at 25.0˚C. Each sorption experiment was performed in 50-mL volumetric flask by mixing a 1.0 mL of 0.1 mol L^{-1} of either Co(II) or Ni(II) ions solution with 100 mg of each biosorbent and the pH was adjusted by adding 9.0 mL of buffer solution. The mixture was shaken for 30 min (200 rpm) to achieve the equilibrium. This mixture was filtered and washed with 50 ml of double distilled water. At equilibrium, the amount of metal remaining in solution became time invariant. The metal content in the filtrate was measured using AAS. The biosorption capacity was calculated from the metal mass balance by Eq. (1).

$$\text{Biosorption capacity} = \frac{(C_0 - C_f)V}{W} \times 1,000 \quad (1)$$

where C_0 and C_f (mM) are the concentrations of the metal ions in the initial and final solutions, V (mL) is the volume of the biosorption reaction, W (g) is the weight of the sorbent, and the biosorption metal capacity (μmol g^{-1}) represents the amount of the metal ions adsorbed per 1.0 g of dry sorbent.

2.4.1. Effect of pH

The previously mentioned batch experiment procedure was carried out at different buffered mixtures (pH 1.0–7.0). The residual metal ions concentration after the biosorption process was determined by AAS and the metal biosorption capacities were then calculated from Eq. (1).

2.4.2. Effect of contact time

The same batch experiment procedure was carried out at different shaking time intervals (1, 5, 10, 15, 20, and 30 min) at the optimum buffering condition. The metal content concentrations were measured by AAS and the biosorption capacity was determined as described before.

2.4.3. Effect of biosorbent dosage

Similar batch experiments were carried out by mixing different sorbent masses (10, 20, 30, 40, and 50 mg) with 1.0 ml of 0.1 M of Co(II) or Ni(II) ions solution and 9.0 mL of buffer solution (pH 6.0 for Co(II) and pH 7.0 for Ni(II)). The biosorption mixture was shaken for 30 min and the residual metal concentration was determined by AAS.

2.4.4. Effect of initial metal ions concentration

Adsorption experiments were carried out at 25˚C by adding 100 mg of each biosorbent to 1 mL of different initial metal ions concentrations (0.01, 0.05, 0.1, 0.25, 0.5, and 1.0 M) and 9.0 mL of buffer. The mixture was shaken for 30 min, then filtered, and washed three times with 50 ml of double distilled water. The residual metal ions concentration was determined by AAS to estimate the metal biosorption capacity.

2.4.5. Effect of interfering ions

The biosorption capacities of Co(II) and Ni(II) were investigated in the presence of different competing metal ions (Na^+, K^+, Ca^{2+}, Mg^{2+}, and Cu^{2+}) under equimolar concentration. The examined solutions were prepared by mixing 100 mg of the each biosorbent with 1.0 mL of 0.1 mol L^{-1} of each metal ion solution in the presence of 1.0 mL of 0.1 mol L^{-1} of each interfering metal ions solution. Then, the pH of the mixture was adjusted by adding 8.0 mL buffer solution (pH 6 for Co(II) and pH 7 for Ni). The biosorption mixture was shaken for 30 min, filtered, and washed three times with 50 mL double distilled water. The residual Co(II) and Ni(II) ions concentration was determined by AAS. For successful comparison, the metal biosorption capacity was evaluated in the absence of the interfering ions.

2.5. Sorption kinetics experiments

Kinetics experiments were carried out at 25°C by mixing 100 mg of Mi or Mi-yeast biosorbent with 1.0 mL of metal ions solution (0.01, 0.05, 0.1, 0.25, 0.5, and 1.0 mol L^{-1}) and 9 mL of buffer. At pre-determined time intervals, the residual metal content, C_t (M) was determined by AAS. The amount, q_t (mg g^{-1}) adsorbed at time t was calculated using Eq. (2). All biosorption experiments were run in triplicate. The difference in results for the triplicates was typically less than 3%.

$$q_t = \frac{(C_0 - C_t)V}{W} \times \text{Atomic mass} \quad (2)$$

2.6. Potential applications for the extraction of Co(II) and Ni(II) from real samples

Different real samples of sea, drinking tap, industrial wastewater, and marine sediment were studied for removing Co(II) or Ni(II) ions by [Mi] and [Mi-yeast]. Wastewater samples were pre-analyzed for the investigated metal cations by AAS. The sea and drinking tap wastewater samples were found to be free from Co(II) and Ni(II) ions and therefore, it was spiked with 1.248, 1.833 mg L^{-1} Co(II) ions and 1.496, 1.864 mg L^{-1} Ni(II) ions, respectively. The industrial wastewater sample was contaminated with 1.026 mg L^{-1} of Co(II) ions and 1.736 mg L^{-1} of Ni(II) ions. Extraction of Co(II) and Ni(II) ions from all samples were carried out by passing a 1-L solution through a micro-column packed with 500 ± 1 mg of each biosorbent under constant flow rate (10 mL min^{-1}). The effluent was collected and analyzed to determine the residual metal ions concentration. The percentages of the metal removal were determined on the basis of triplicate analysis.

3. Results and discussion

3.1. SEM analysis of Mi and Mi-yeast biosorbents

SEM images shown in Fig. 1(a) and (b) enable direct observation of the surface microstructures and comparison between Mi and Mi-yeast. It has been concluded that Mi is a compact fibrous material with a mixture of mesopores (pore diameter ranging from 2 to 50 μm) and macropores (pore diameter > 50 μm), while the micrographs of Mi-yeast revealed the presence of irregular particles with heterogeneous structures with more internal binding sites to adsorb more Co(II) and Ni(II) ions [31].

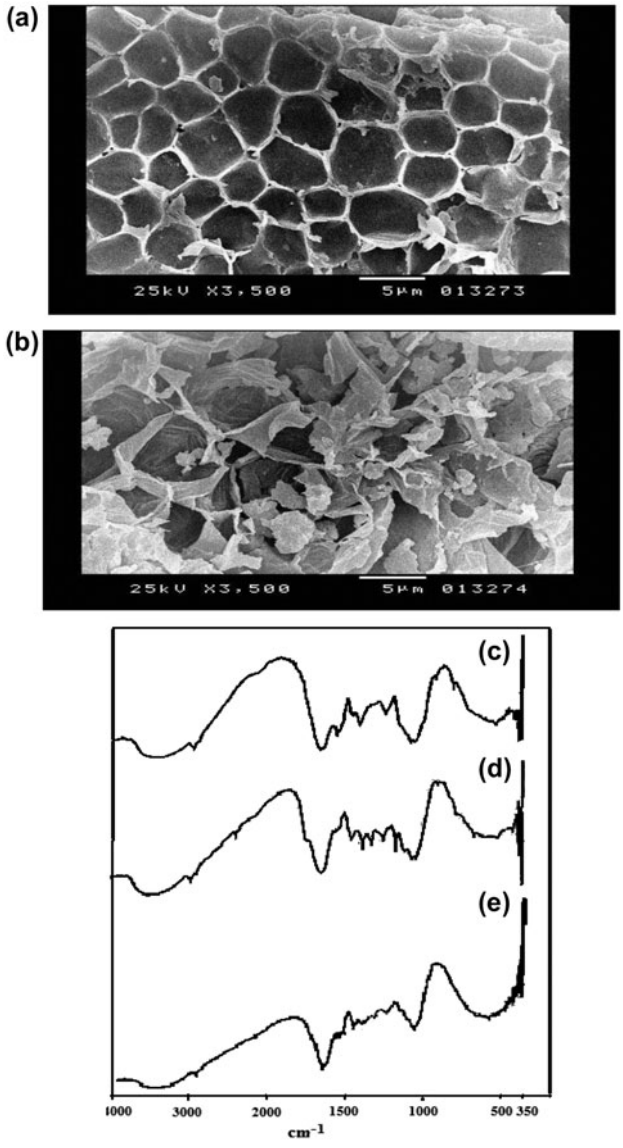

Fig. 1. Characterization of the synthesized biosorbents (a) SEM image for Mi (b) SEM image for Mi-yeast (c) FTIR of yeast (d) FTIR of Mi and (e) FTIR of Mi-yeast.

3.2. FTIR characterization

A biosorbent may consist of complex organic materials such as proteins, lipids, and carbohydrate polymers. Biosorption mostly depends on the available functional groups in a particular biosorbent. The FTIR spectra of baker's yeast as a modifier, Mi, and Mi-yeast are shown in Fig. 1(c–e), respectively. The broad intense peaks located at 3,430 cm^{-1} for baker's yeast, 3,472 cm^{-1} for Mi and 3,405 cm^{-1} for Mi-yeast correspond to the fundamental stretching vibrations of different types of free hydroxyl groups [32,33]. The peaks at 2,921–2,931 cm^{-1} for yeast, Mi, and Mi-yeast

correspond to the symmetric or asymmetric (υ_{C-H}) of aliphatic acids [34]. The peak observed at 2,353–2,358 cm^{-1} for Mi and Mi-yeast corresponds to (υ_{C-H}) stretching which is absent in yeast [35]. Asymmetric (υ_{COO^-}) stretching vibration is observed at 1,657 cm^{-1} for yeast, at 1,632 cm^{-1} for Mi, and at 1,651 cm^{-1} for Mi-yeast while the peaks correspond to symmetric (υ_{COO^-}) are observed at 1,407 cm^{-1} for yeast, 1,451 cm^{-1} for Mi and 1,454 cm^{-1} for Mi-yeast suggesting the interaction between the Mi and the yeast [33]. The peak observed at 1,318 cm^{-1} for Mi and absent in yeast and Mi-yeast may be assigned to symmetric stretching (υ_{COOR}) [36]. The aliphatic acid group vibration at 1,240 cm^{-1} for yeast, at 1,280 cm^{-1} for Mi, and at 1,242 cm^{-1} for Mi-yeast correspond to deformation vibration of C=O and stretching formation of O–H of carboxylic acid and phenols [37]. The stretching (υ_{C}–OH) of alcoholic and carboxylic acid groups is observed at 1,076 cm^{-1} for yeast, 1,067 and 1,166 cm^{-1} for Mi, and at 1,067 cm^{-1} for Mi-yeast. Generally, the peaks detected in the range 1,170–1,000 cm^{-1} are assigned for (υ_{COC}), (υ_{COP}) and (υ_{OH}) of polysaccharides [38]. The peaks observed at 918 and 1,551 cm^{-1} for yeast are suggested to be interactive binding sites between yeast and Mi that are absent in Mi-yeast. However, the additional peaks at 610 cm^{-1} for Mi and 594 cm^{-1} for Mi-yeast can be assigned to bending modes of aromatic compounds [39]. It is concluded that –COOH and –OH groups in Mi and Mi-yeast may function as proton donors and hence the deprotonation of those groups may be involved in binding to metal ions [40].

3.3. Effect of pH

The biosorption medium pH is a key factor for controlling the number of biosorbent surface sites available to bind metal cations. The effect of pH on biosorption of Co(II) and Ni(II) ions onto Mi and Mi-yeast biosorbents was examined in pH range of 1.0–7.0, Fig. 2(a). Experiments could not be conducted beyond pH 7.0 due to metal precipitation. Generally, the biosorption capacity of Mi and Mi-yeast increased with increasing pH to a maximum value at pH 6.0 for Co(II) and pH 7.0 for Ni(II) ions. The enhanced biosorptive capacity of Mi-yeast compared to Mi may be explained by the increase in the availability of binding sites and improvement in the access of metal ions to its metal binding sites. The biosorbent surface is regarded as a mosaic of different negatively charged functional groups that can bind to metal ions via various mechanisms. At pH values above the isoelectric point, the net negative charges on the cell wall components and

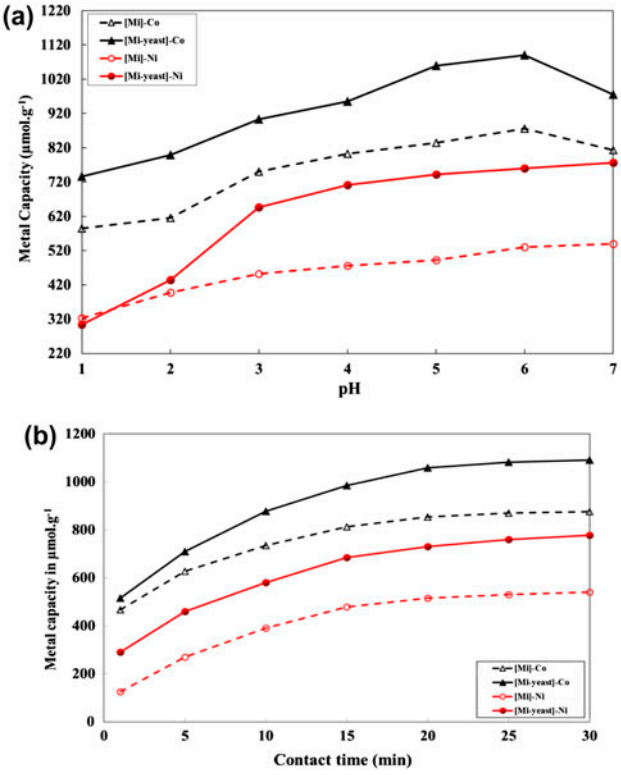

Fig. 2. Factors affecting the sorption capacities of Co(II) and Ni(II) by Mi and Mi-yeast biosorbents (a) effect of pH and (b) effect of contact time at pH 6 for Co(II) and pH 7 for Ni(II).

carboxyl, phosphate, and amino ligands will promote reaction with metal ions via hydrogen bonding mechanism, Eq. (3) and ion exchange [41]. As the pH is lowered, however, the overall surface charge on the cells will be positive, which inhibits the approach of metal ions as a result of repulsive forces leading to biosorption inhibition [42]. Also, Co(II) or Ni(II) ions may compete with hydrogen ions and thus the biosorption process is mainly performed by ion-exchange mechanism [43–46]. The binding of metal ions to Mi-yeast functional groups can be proceed via complex formation and/or ion-exchange mechanisms, Eqs. (4) and (5).

$$2(\text{Mi-yeast}) - \text{COOH} + \text{M(OH)}_2 \rightarrow (\text{Mi-yeast} - \text{COOH})_2\text{M(OH)}_2 \quad (3)$$

$$2(\text{Mi-yeast}) - \text{COOH} + \text{M}^{2+} \rightarrow (\text{Mi-yeast} - \text{COO})_2\text{M} + 2\text{H}^+ \quad (4)$$

$$(\text{Mi-yeast}) - \text{COOH} + \text{M(OH)}^+ \rightarrow \text{Mi-yeast} - \text{COO} - \text{M(OH)} + \text{H}^+ \quad (5)$$

3.4. Effect of contact time

The effect of contact time is important to identify the binding rate of Co(II) and Ni(II) ions to Mi and Mi-yeast and certify the optimum time for complete metal removal. The biosorption experiments were carried out for different contact times (1, 5, 10, 15, 20, 25, and 30 min) with fixed amount of biosorbent at 25°C, Fig. 2(b). Co(II) ions show higher biosorption capacity than Ni(II) for both Mi and Mi-yeast. The metal uptake processes were found to proceed with high rates after 5.0 min of shaking time, where the interaction between both metal ions and biosorbents was taken place in two successive steps. The first step proceed via a gradual increase up to 80% extraction percentage during the first 10 min and this trend refers to the fast equilibration and kinetics of the biosorption process. The second step is based on complete saturation of biosorbents surfaces with the metal cations. The biosorption equilibrium was established in 30 min.

3.5. Effect of biosorbent dosage

The effect of Mi or Mi-yeast dosage on the biosorption capacity of Co(II) or Ni(II) was investigated at pH 6 for Co(II), pH 7 for Ni(II), and 25°C using different biosorbent doses (10–400 mg) and initial metal ions concentration (0.10 mol L^{-1}), as shown in Table 1. The biosorption capacity increased as the biosorbent dose increased. The maximum biosorption capacity values were achieved when 100 mg biosorbent dose was used. Further increase in the biosorbent mass showed no significant increase in the metal biosorption capacity.

3.6. Biosorption isotherms

Biosorption isotherms describe the equilibrium distribution of adsorbed molecules between the solid and liquid phases. Different equilibrium adsorption isotherm models can be applied to give an obvious behavior of biosorbents with metal ions. The concentration variation method is commonly used to calculate the adsorption constants and characteristics of both biosorbents and biosorption process. Generally, the biosorption equilibrium condition is recognized when the concentration of sorbate in the bulk solution is in a dynamic balance with that of the solid/liquid interface. Equilibrium batch experiments were carried out with different initial metal concentrations (0.01–1.0 mol L^{-1}) for 30 min contact time and 100 mg of dry Mi and Mi-yeast sorbents at pH 6.0 for Co(II) and pH 7.0 for Ni(II). The mixture was filtered and washed three times with 50 ml of double distilled water. The residual metal concentration was determined by AAS. The metal biosorption capacity and percent biosorption at each initial concentration were then determined. The elucidation of isotherm data by fitting them to different models is a substantial step in the adsorption study. The present biosorption data of Co(II) and Ni(II) sorbed onto Mi and Mi-yeast are tested by Langmuir, Freundlich, and Dubinin–Radushkevich isotherm models to recognize the best model that fit the experimental data and to provide information about the effectiveness of the metal–sorbent system.

3.6.1. Freundlich adsorption model

Freundlich was the first to propose an empirical formula describing the adsorption isotherm [47]. It assumed that different adsorption sites exist on the solid phase surface with different adsorption energy to interact with adsorbed species. This model is often used for adsorbents with an irregular surface or single solute systems within a specific concentration range. Also, it is used to estimate the adsorption intensity towards the adsorbate on a heterogeneous energetic distribution of active binding sites of adsorbent. The Freundlich equation is expressed by Eq. (6).

Table 1
Effect of biosorbent dosage on Co(II) and Ni(II) capacity under optimum buffering conditions (pH 6 for Co(II) and pH 7 for Ni(II))

	Co(II)		Ni(II)	
Biosorbent dosage (mg)	[Mi]	[Mi-yeast]	[Mi]	[Mi-yeast]
10	81	89	48	72
25	205	254	123	185
50	420	510	256	367
100	876	1,091	540	777
200	1,012	1,358	775	960
400	1,380	1980	1,062	1,250

$$q_e = K_F C_e^{\frac{1}{n}} \quad (6)$$

where q_e is the amount adsorbed (mg) per one gram of the adsorbent, C_e is the equilibrium concentration (mg L^{-1}), while K_F and n are constants. K_F is the function of adsorption energy and temperature and measures the adsorptive capacity and n determines the intensity of adsorption or the adsorbent–adsorbate bond strength and can help determine whether adsorption is favored. The value $n > 1$ describes favorable adsorption, whereas $n = 1$ characterizes linear adsorption and $n < 1$ describes unfavorable adsorption situations. The linear form of Freundlich isotherm is shown in Eq. (7).

$$\log q_e = \frac{1}{n}\log C_e + \log K_F \quad (7)$$

According to Freundlich model, the values of K_F and n, Table 2 for Mi and Mi-yeast biosorbents can be obtained from the slope and intercept of the linear plots of Eq. (7). It is concluded from Table 2 that the calculated values of $n > 1$ reveal that adsorption is favorable.

The sorption constant, K_F increased upon immobilization of yeast on Mi and thus, Mi-yeast showed higher maximum biosorption capacity and faster biosorption equilibrium compared to the native biosorbent. Moreover, the high values of R^2 revealed that the Freundlich isotherm model is suitable for describing the adsorption behavior in this study.

3.6.2. Langmuir adsorption model

Langmuir model is the most commonly used isotherm for sorption of solute onto a solid surface due to its simplicity and good agreement with experimental data. This model assumed a reversible sorption process on uniform adsorbent surface, with limited adsorption sites, forming a monolayer sorption without interactions between the adsorbed species. In addition, adsorbate molecules occupying separate surface sites, do not interact with each other and have equal affinity and uniform sorption energies [48]. The Langmuir isotherm equation is given by Eq. (8).

$$q_e = \frac{K_L q_{max} C_e}{1 + K_L C_e} \quad (8)$$

where C_e (mg L^{-1}) describes the equilibrium Co(II) or Ni(II) ions concentration, q_e (mg g^{-1}) is the amount of Co(II) or Ni(II) cations adsorbed on Mi or Mi-yeast surface at equilibrium, q_{max} (mg g^{-1}) is the maximum adsorption capacity corresponding to complete monolayer coverage, and K_L (L mg^{-1}) is the Langmuir adsorption constant (adsorption affinity constant). Accordingly, the experimental adsorption data converge to horizontal plateaus. Each plateau corresponds to the formation of a monolayer of adsorbent on the Mi or Mi-yeast surfaces. The linearized form of Langmuir isotherm is represented by Eq. (9).

$$\frac{C_e}{q_e} = \frac{C_e}{q_{max}} + \frac{1}{K_L q_{max}} \quad (9)$$

The values of q_{max} and K_L in Table 2, calculated from the slope and intercept of linear plots of C_e/q_e vs. C_e. were found to increase upon immobilization of yeast on Mi as revealed from their higher values of maximum biosorption capacity (526 mg g^{-1} for Co(II) and 250 mg g^{-1} for Ni(II)). The order of the biosorption capacity was found as Co(II) > Ni(II), which indicates that the biosorbents have more affinity to Co(II) compared to Ni(II) ions. The equilibrium constants K_L tend to decrease on going from Mi to Mi-yeast for both metal ions. The essential characteristics of the Langmuir isotherms may be expressed in terms of dimensionless separation factor F_L as in Eq. (10) [49–51]. The F_L value indicates the adsorption nature to be unfavorable if $F_L > 1$, linear if $F_L = 1$, favorable if $0 < F_L < 0$, and irreversible if $F_L = 0$. All calculated F_L

Table 2
Different adsorption isotherm parameters for Pb(II) and Cd(II) onto Mi and Mi-yeast at 25°C and optimum pH values

		Langmuir model			Freundlich model			Dubinin–Radushkevich model			
Metal ion	Sorbent	q_{max} (mg g^{-1})	$K_L \times 10^{-5}$	R^2	K_F	n	R^2	q_D (mg g^{-1})	B_D	E_D (kJ/mol)	R^2
Co(II)	[Mi]	435	9.43	0.965	0.150	1.29	0.969	99.5	0.0062	7.9	0.643
	[Mi-yeast]	526	8.68	0.989	0.459	1.41	0.951	117.8	0.0064	7.8	0.562
Ni(II)	[Mi]	227	6.35	0.958	0.046	1.24	0.953	64.5	0.0349	3.8	0.608
	[Mi-yeast]	250	1.57	0.978	0.197	1.39	0.896	87.3	0.0012	6.2	0.687

values Table 2 were found to be from 0.74 to 5.6×10^{-6} for the initial concentrations range 2.12×10^{3}–2.07×10^{5} mg L^{-1} of metal ions, indicating favorable biosorption processes. In addition, the R^2 values (≈1.0) proving that the biosorption data fitted well to Langmuir isotherm model and suggest the homogeneous monolayer biosorption.

$$F_L = \frac{1}{1 + K_L C_0} \tag{10}$$

3.6.3. Dubinin–Radushkevich (D–R) isotherm model

D–R isotherm is an empirical model initially conceived for the adsorption of subcritical vapors onto micropore solids following a pore filling mechanism [52]. It is often used to estimate the characteristic porosity in addition to the apparent free energy of adsorption. This model is valid at low or intermediate concentration ranges and can be used to describe the adsorption mechanism with a Gaussian energy distribution onto heterogeneous surface [53–55]. The D–R equation can be expressed by Eq. (11).

$$q_e = q_D \exp\left(-B_D\left[RT \ln\left(1 + \frac{1}{C_e}\right)\right]^2\right) \tag{11}$$

where q_D (mg g^{-1}) is the D–R constant which is related to monolayer sorption capacity by Mi or Mi-yeast surface. B_D (mol^2 J^{-2}) is the constant related to the sorption mean free energy, E_D (kJ mol^{-1}) of Co(II) or Ni(II) when it is transferred from infinity to the sorbent surface in solution, R (8.31 J mol^{-1} K^{-1}) is the ideal gas constant, and T (K) is the absolute temperature.

The linear form of Eq. (11) is given by Eq. (12).

$$\ln q_e = \ln q_D - B_D\left[RT \ln\left(1 + \frac{1}{C_e}\right)\right]^2 \tag{12}$$

The value of mean sorption free energy, E (J mol^{-1}) is defined as the free energy change required to transfer 1 mol of ions from solution to the solid surfaces and can be calculated from D–R parameter B_D according to Eq. (13) [56].

$$E = \frac{1}{\sqrt{2B_D}} \tag{13}$$

The values of q_D and B_D for D–R model, evaluated from the intercepts and slopes of the linear plots of $\ln q_e$ against $[RT \ln(1 + 1/C_e)]^2$ for the biosorption of Co(II) and Ni(II) by Mi and Mi-yeast are collected in Table 2. The D–R approach is usually applied to give information about the type of adsorption mechanism as chemical ion-exchange or physical adsorption based on the value of mean free energy, E. If the magnitude of E is between 8 and 16 kJ mol^{-1}, the sorption process is supposed to proceed via chemisorption (chemical ion-exchange processes), while if the values of $E < 8$ kJ mol^{-1}, the sorption process is of physical nature and finally if the values of $E > 16$ kJ mol^{-1}, the adsorption mechanism may be dominated by particle diffusion. [57–60]. The calculated values of mean free energy, E for both adsorbents were <8 kJ mol^{-1}, indicating that the biosorption processes of Co(II) and Ni(II) by Mi and Mi-yeast are of physisorption nature. The D–R isotherm model shows an inadequate fit of experimental data in the whole range of concentrations giving the lowest R^2 values (0.562–0.687) among the applied models. The poor ability of this model to represents the experimental data could be due to the homogeneity of the adsorbent surface. In summary, the biosorption of Co(II) and Ni(II) by Mi and Mi-yeast is favorable and Langmuir isotherm model best fits the experimental data compared to Freundlich and D–R models.

3.7. Kinetic studies

A suitable kinetic model is imperative to analyze data of biosorption rate and to examine the mechanism of biosorption process. Different models were used to analyze the kinetic data of Co(II) and Ni(II) onto the Mi and Mi-yeast. Lagergren pseudo-first-order, pseudo-second-order [61,62], Elovich [63], and intraparticle diffusion [64] kinetics models were applied to fit the experimental data. All the kinetic equations and their parameters are shown in Table 3, where q_e and q_t are the biosorption capacity (mg g^{-1}) at equilibrium and at time t (min), respectively, k is the rate constant, and R^2 is the correlation coefficients to express the uniformity between the experimental data and model predicted values. From the slope of Fig. 3(a), the Lagergren-first-order rate constants k_1 can be obtained. The correlation coefficients R^2 (0.886–0.967) and the predicted q_e values for the first-order kinetic model did not give reasonable values, suggesting that the adsorption system is not a first-order reaction. The pseudo-second-order kinetic constant k_2 and q_e can be calculated from the intercept and slope of plots of t/q_t vs. t, Fig. 3(b). The calculated k_2, q_e, and

Table 3
Kinetic equations that used to analyze the adsorption of Co(II) and Ni(II) on Mi and Mi-yeast biosorbents

Kinetic models	Linear kinetic equations	Plot	Slope	Intercept	Calculated parameters
Lagergren pseudo- first-order	$\ln(q_e - q_t) = \ln q_e - K_1 t$	$\ln(q_e - q_t)$ vs. t	K_1	$\ln q_e$	q_e(mg g^{-1}) , K_1 (min^{-1})
Pseudo-second-order	$\frac{t}{q_t} = \frac{1}{K_2 q_e^2} + \frac{t}{q_e}$	$\frac{t}{q_t}$ vs. t	$\frac{1}{q_e}$	$\frac{1}{K_2 q_e^2}$	q_e(mg g^{-1}) , K_2(g mg^{-1} min^{-1})
Elovich	$q_t = \frac{1}{\beta}\ln(\alpha\beta) + \frac{1}{\beta}\ln t$	q_t vs. $\ln t$	$\frac{1}{\beta}$	$\frac{1}{\beta}\ln(\alpha\beta)$	q_e(mg g^{-1}), α(mg g^{-1} min^{-2}), β(g mg^{-1} min^{-1})
Intraparticle diffusion	$q_t = K_{int}\sqrt{t} + C$	q_t vs. $\sqrt{t}$	K_{int}	C	q_e(mg g^{-1}), K_{int}(mg g^{-1} min$^{-1/2}$)

R^2 in Table 4 showed a good agreement with the pseudo-second-order model which suggests that the rate-limiting step in biosorption is controlled by chemical process [65]. The Elovich equation used to interpret the predominantly chemical biosorption on highly heterogeneous adsorbents was also adopted to fit the experimental data. Where α is the initial adsorption rate (mg g^{-1} min^{-2}) and β is the desorption constant (g mg^{-1} min^{-1}) related to the extent of surface coverage and activation energy for chemisorption. The Elovich constants, α and β are calculated and given in Table 4. The plots of q_t vs. ln(t) in Fig. 3(c) display a good linear relationship before reaching the biosorption equilibrium. However, the correlation coefficients are lower than those of the pseudo-second-order equation and the calculated q_e values do not agree with the experimental data. This means that the biosorptions of Co(II) and Ni(II) onto Mi and Mi-yeast are not highly heterogeneous systems. The intraparticle diffusion equation describes the movement of ions from bulk solution to the solid phase. Where k_{int} is the intraparticle diffusion rate constant (mg g^{-1} min$^{-1/2}$) which can be obtained from the slope of straight line of plots of q_t vs. $t^{1/2}$, Fig. 3(d). The constant C is related to the boundary layer thickness (mg g^{-1}) which can be deduced from the intercept of straight lines. The constants k_{int} and C are calculated and given in Table 4. All C values are not equal to zero indicating that the adsorption process may not be mainly controlled by intraparticle diffusion [66]. From all the correlation coefficients (R^2) and above analysis, it is concluded that the pseudo-second order is the most suitable kinetics model for biosorption of Co(II) and Ni(II) onto Mi and Mi-yeast biosorbents.

3.8. Effect of interfering ions

The effect of the presence of equimolar concentrations of metal ions and Na^+, K^+, Ca^{2+}, or Mg^{2+} as interfering ions on the biosorption capacity was investigated for Mi and Mi-yeast. The results of this study are listed in Table 5. Comparing the biosorption capacity of Co(II) and Ni(II) ions in the presence and absence of interfering ions, showed that K^+ and Mg^{2+} have minimum inference relative to Ca^{2+} and Na^+. The difference in the affinity of these interfering ions for competing on the biosorption sites is influenced by the difference in charge and size of the hydrated ions, as well as the nature of functional groups present on yeast [67].

3.9. Desorption and reuse of the biosorbents

The regeneration of the biosorbents is an important controlling parameter in assessing their potential for commercial applications. Desorption of Co(II), and Ni(II) from the metal-loaded Mi and Mi-yeast was performed using 0.2 M HCl [68]. In order to show the reusability of the biosorbents, adsorption–desorption cycle of Co(II) and Ni(II) was repeated five times using the same preparations. The biosorption efficiency of both biosorbents did not noticeably change and only a maximum 4.0–7.0% decrease was observed after five cycles. This may be due to the small amount of biomass lost during the repeated adsorption–desorption operations.

3.10. Thermodynamic study

The effect of temperature on the equilibrium constants of the biosorption of Co(II) and Ni(II) ions onto Mi-yeast was investigated. The thermodynamic parameters, free energy change (ΔG), enthalpy change (ΔH), and entropy change (ΔS) were calculated using Eq. (14).

$$\ln K = \frac{-\Delta G^\circ}{RT} = \frac{\Delta S^\circ}{R} - \frac{\Delta H^\circ}{RT} \quad (14)$$

where R is the ideal gas constant (8.3145 J mol^{-1} K^{-1}), T is the absolute temperature (K), and K is the conditional equilibrium constant for the investigated adsorption

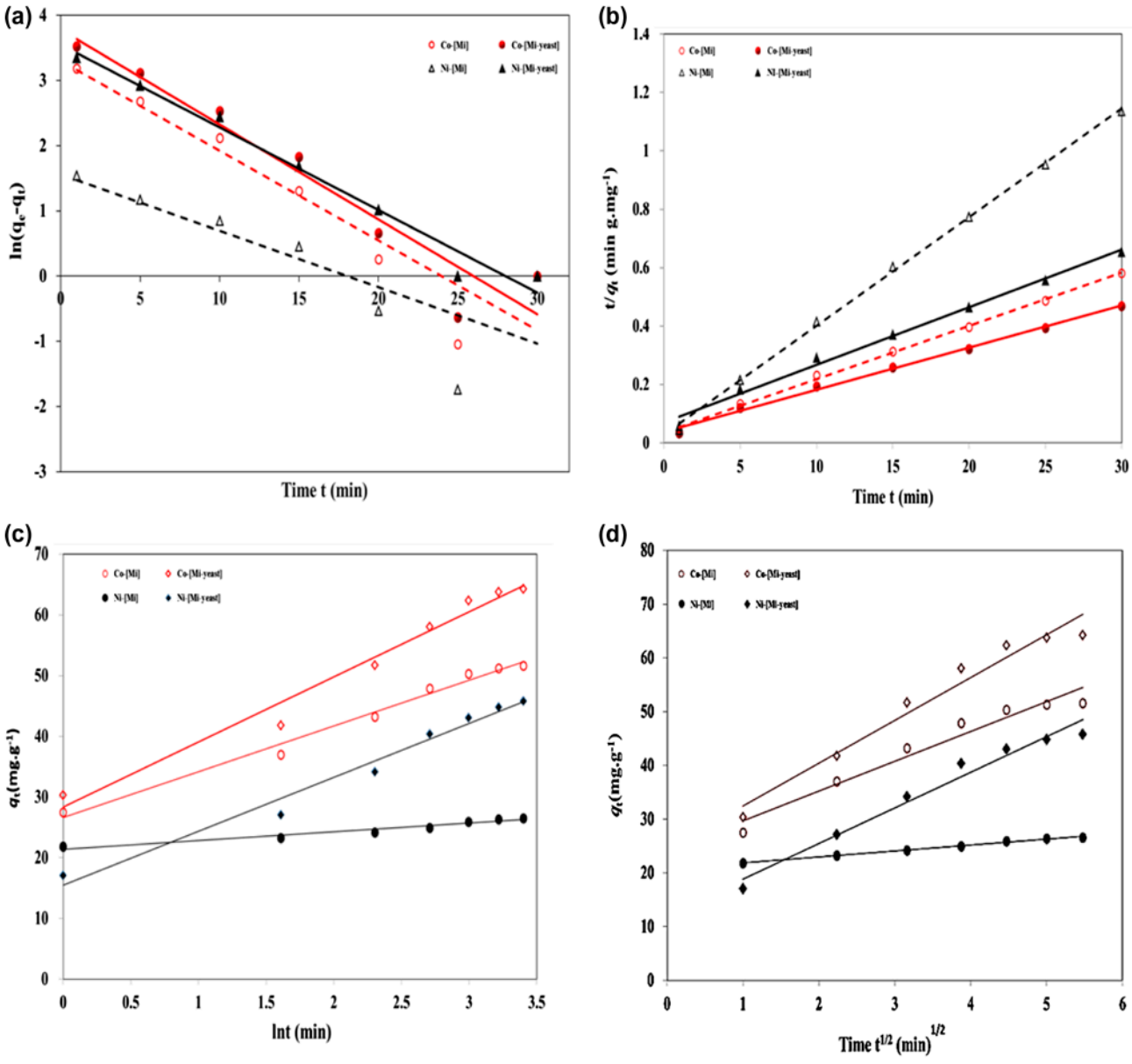

Fig. 3. Fitting of kinetic models (a) Lagergren pseudo-first order, (b) pseudo-second order, (c) Elovich and (d) intraparticle diffusion for the biosorption of Co(II) and Ni(II) on Mi and Mi-yeast biosorbents at initial concentration of 0.10 mol L^{-1} at 25°C.

processes. The adsorption experiments were repeated at three different temperatures 15, 25, and 35°C using 0.10 M solutions of Co(II) ions at pH 6.0 and Ni(II) ions at pH 7.0 and 100 mg biosorbent dose. The calculated values of ΔG were –1.24 and –2.58 kJ mol^{-1} for Co(II) and Ni(II)-adsorption systems, respectively, indicating feasible biosorption processes. Additionally, the ΔH values were 9.54 and 6.58 kJ mol^{-1} for the adsorption cases of Co(II) and Ni(II) ions, respectively, representing the endothermic nature of the biosorption. Finally, the evaluated positive ΔH values for Co(II) and Ni(II)-adsorption systems (51.91 and 34.93 J K^{-1} mol^{-1}, respectively) assure the increase in the order of the metal–Mi-yeast bound products because of the good ability for the metal ions to complex Mi-yeast functional groups.

3.11. Applications of Mi and Mi-yeast for Co(II) and Ni(II) extraction from real water samples

The applications of Mi and Mi-yeast for biosorptive removal of Co(II) and Ni(II) from real wastewater

Table 4
Kinetic parameters used to analyze the adsorption of Pb(II) and Cd(II) on Mi and Mi-yeast biosorbents

Kinetic models and parameters	Co(II) [Mi-yeast] ([Mi])						Ni(II) [Mi-yeast] ([Mi])					
	0.01 mol/L	0.05 mol/L	0.10 mol/L	0.25 mol/L	0.50 mol/L	1.0 mol/L	0.01 mol/L	0.05 mol/L	0.10 mol/L	0.25 mol/L	0.50 mol/L	1.0 mol/L
q_e (exp.) (mg g^{-1})	6.75	33.63	64.03	159.64	319.87	635.64	4.578	23.01	45.60	113.4	225.4	448.1
	(5.28)	(26.65)	(51.42)	(129.7)	(257.8)	(511.2)	(2.641)	(13.21)	(26.41)	(66.03)	(132.1)	(264.1)
Pseudo-first order												
q_e (calc.) (mg g^{-1})	4.81	33.63	64.03	159.64	319.8	635.6	3.078	23.00	34.83	118.9	267.0	497.0
	(3.110)	(22.78)	(27.14)	(89.38)	(198.9)	(543.9)	(0.692)	(3.462)	(4.756)	(17.31)	(34.62)	(69.25)
K_1 (min^{-1})	0.130	0.177	0.146	0.171	0.166	0.218	0.1211	0.1615	0.266	0.257	0.271	0.288
	(0.147)	(0.177)	(0.138)	(0.156)	(0.182)	(0.235)	(0.130)	(0.130)	(0.0863)	(0.130)	(0.130)	(0.130)
R^2	0.979	0.894	0.928	0.957	0.969	0.897	0.966	0.938	0.978	0.894	0.877	0.931
	(0.974)	(0.894)	(0.886)	(0.976)	(0.957)	(0.912)	(0.927)	(0.927)	(0.661)	(0.927)	(0.927)	(0.927)
Pseudo-second order												
q_e (calc.) (mg g^{-1})	7.14	34.48	66.22	166.7	322.7	625.0	4.968	25.77	45.45	112.4	222.2	454.5
	(5.59)	(26.32)	(52.63)	(129.9)	(263.2)	(526.3)	(2.687)	(13.44)	(26.88)	(66.67)	(135.1)	(270.3)
K_2 (min^{-1}) × 10^{-3}	0.051	0.0093	6.1×10^{-3}	2.5×10^{-3}	1.3×10^{-3}	7.1×10^{-4}	0.067	0.011	6.9×10^{-3}	2.9×10^{-3}	1.4×10^{-3}	7.2×10^{-3}
	(0.098)	(0.0178)	(0.0103)	(3.9×10^{-3})	(2.0×10^{-3})	(1.0×10^{-3})	(0.456)	(0.097)	(0.0486)	(0.0148)	(9.6×10^{-3})	(4.7×10^{-3})
R^2	0.995	0.988	0.995	0.996	0.996	0.995	0.989	0.991	0.992	0.992	0.992	0.994
	(0.998)	(0.995)	(0.997)	(0.997)	(0.997)	(0.997)	(0.999)	(0.999)	(0.999)	(0.996)	(0.999)	(0.999)
Elovich												
q_e (calc.) (mg g^{-1})	3.086	19.73	41.03	122.7	278.0	426.4	2.210	13.46	30.84	94.22	217.2	497.3
	(2.867)	(14.64)	(30.45)	(86.14)	(190.8)	(616.7)	(2.141)	(10.70)	(21.41)	(53.52)	(107.0)	(214.1)
α (mg g^{-1}.min^{-2})	11.51	52.86	151.7	365.5	736.6	2,352	16.13	23.99	50.81	131.6	254.87	505.8
	(34.17)	(114.2)	(260.0)	(575.2)	(1,209)	(1,551)	(4.6×10^5)	(2.3×10^6)	(4.6×10^5)	(1.1×10^7)	(2.3×10^7)	(4.6×10^7)
β (g mg^{-1} min^{-1})	0.836	0.1667	0.093	0.037	0.0186	0.0130	1.470	0.218	0.1126	0.0454	0.0227	0.0113
	(1.353)	(0.2532)	(0.1328)	(0.0519)	(0.0261)	(0.0094)	(6.700)	(1.400)	(0.700)	(0.300)	(0.140)	(0.070)
R^2	0.991	0.957	0.975	0.986	0.979	0.985	0.884	0.980	0.978	0.984	0.974	0.984
	(0.973)	(0.967)	(0.986)	(0.984)	(0.987)	(0.978)	(0.946)	(0.946)	(0.946)	(0.946)	(0.946)	(0.946)
Intraparticle diffusion												
q_e (calc.) (mg g^{-1})	6.25	25.0	60.12	150.2	300.4	599.5	4.193	21.15	41.82	104.7	208.2	417.3
	(5.020)	(30.91)	(48.94)	(122.5)	(245.4)	(489.1)	(2.570)	(12.84)	(25.67)	(64.18)	(128.4)	(256.7)
K_{int} (mg g^{-1} $min^{-1/2}$)$^{-3}$	0.882	2.964	7.961	19.89	39.92	78.77	0.529	3.404	6.618	16.31	32.91	65.62
	(0.5446)	(4.532)	(5.537)	(14.62)	(28.12)	(56.18)	(0.110)	(0.547)	(1.094)	(2.736)	(5.472)	(10.94)
C	2.304	11.77	24.52	61.27	121.9	247.3	1.825	5.931	12.22	31.71	61.05	123.8
	(2.584)	(10.65)	(24.18)	(58.70)	(119.6)	(237.9)	(2.078)	(10.39)	(20.78)	(51.95)	(103.9)	(207.8)
R^2	0.962	0.974	0.964	0.957	0.961	0.961	0.955	0.969	0.972	0.963	0.969	0.961
	(0.944)	(0.974)	(0.952)	(0.964)	(0.952)	(0.944)	(0.991)	(0.991)	(0.991)	(0.991)	(0.991)	(0.991)

Table 5
Co(II) and Ni(II) sorption capacities (μmol g^{-1}) in the presence of other competing interfering ions under optimum buffering conditions

Biosorbent		Na^+	K^+	Mg^+	Ca^+	Cu^{2+}
	Co(II) biosorption capacity	Co(II) biosorption capacity in presence of interfering ions				
[Mi]	876	835	864	860	794	758
[Mi-yeast]	1,091	1,025	1,078	1,070	1,010	984
	Ni(II) biosorption capacity	Ni(II) biosorption capacity in presence of interfering ions				
[Mi]	540	490	536	528	477	428
[Mi-yeast]	777	742	780	765	718	690

Table 6
Selective solid phase extraction of Co(II) and Ni(II) from different wastewater samples by 500 mg of Mi and Mi-yeast

Wastewater sample	(μg mL^{-1}) spiked (detected)	Co(II) (amount detected) percentage extraction		(μg mL^{-1}) spiked (detected)	Ni(II) (amount detected) percentage extraction	
		[Mi]	[Mi-yeast]		[Mi]	[Mi-yeast]
Tap water	1.833	(0.2065) 88.73% ± 1.9	(0.0573) 96.87% ± 2.3	1.864	(0.1837) 90.14% ± 2.3	(0.1187) 93.63% ± 1.4
Sea water	1.248	(0.2122) 83.00% ± 2.4	(0.0864) 93.08% ± 1.7	1.496	(0.1245) 91.68% ± 2.6	(0.0985) 93.42% ± 2.5
Industrial water	1.026	(0.1125) 89.04% ± 1.8	(0.0438) 95.73% ± 2.1	1.736	(0.1562) 91.00% ± 2.5	(0.0887) 94.89% ± 3.2

samples either contaminated or spiked are summarized in Table 6. The percentages of metal extraction from tap and sea water samples spiked with 1.55–1.76 μg mL^{-1} were found to be in the range of 89.5–92.5% for Co(II), 92.5–93.2% for Ni(II) by Mi-yeast, and 83.4–86.2% for Co(II), and 88.2–89.7% for Ni(II) by Mi. While the percentages of Co(II) and Ni(II) ions from industrial wastewater samples contaminated with 1.03–1.14 μg mL^{-1} are found to be in the range of 95.9–96.6% for Mi-yeast and 91.7–92.9% for Mi. In addition, the percentage extraction of Co(II) from marine sediment contaminated with 1.283 μg mL^{-1} of Cd(II) was found to be 87.8% for the Mi and 91.9% for Mi-yeast. On the other hand, the percentage values of extraction from the industrial wastewater sample were relatively lower than the other two water samples due to the possibility of high contamination of the industrial sample with other competitive interfering ions.

4. Conclusions

The biosorption properties of Mi-yeast were extensively studied for the removal of Co(II) and Ni(II) and compared to the native leaves. Different analytical parameters affecting their sorptive capacities were investigated. Among various isotherm models, the experimental biosorption data best followed the Langmuir isotherm, where the maximum biosorption capacities were 526 mg g^{-1} for Co(II) at pH 6.0 and 250 mg g^{-1} at for Ni(II) at pH 7.0. The kinetic study revealed that the biosorption processes obeyed the pseudo-second-order model, and the adsorption equilibrium could be achieved in 30 min at 25°C. The presence of Na^+, K^+, Ca^{2+}, Mg^{2+}, and Cu^{2+} as interfering ions has a negligible effect on the biosorption performance. The biosorption–desorption studies indicated that Mi-yeast had a high stability and good reusability. The removal efficiencies of spiked Co(II) and Ni(II) ions from real wastewater samples were successfully accomplished (83.0–96.9 ± 1.7–2.4% and 90.1–94.9 ± 1.4–3.2%, respectively). The aforementioned results concluded that Mi-yeast is effective, low-cost, reusable, and eco-friendly biosorbent.

References

[1] C.G. Fraga, Relevance, essentiality and toxicity of trace elements in human health, Mol. Aspects Med. 26 (2005) 235–244.

[2] J. Wang, C. Chen, Biosorption of heavy metals by *Saccharomyces cerevisiae*: A review, Biotechnol. Adv. 24 (2006) 427–451.
[3] P.C. Nagajyoti, K.D. Lee, T.V.M. Sreekanth, Heavy metals, occurrence and toxicity for plants: A review, Environ. Chem. Lett. 8 (2010) 199–216.
[4] B. Volesky, Biosorption and me, Water Res. 41 (2007) 4017–4029.
[5] S. Qaiser, A.R. Saleemi, M. Umar, Biosorption of lead from aqueous solution by *Ficus religiosa* leaves: Batch and column study, J. Hazard. Mater. 166 (2009) 998–1005.
[6] M.M. Matlock, B.S. Howerton, D.A. Atwood, Chemical precipitation of heavy metals from acid mine drainage, Water Res. 36 (2002) 4757–4764.
[7] C. Blöcher, J. Dorda, V. Mavrov, H. Chmiel, N.K. Lazaridis, K.A. Matis, Hybrid flotation membrane filtration process for the removal of heavy metal ions from wastewater, Water Res. 37 (2003) 4018–4026.
[8] S. Rengaraj, C.K. Joo, Y. Kim, J. Yi, Kinetics of removal of chromium from water and electronic process wastewater by ion exchange resins: 1200H, 1500H and IRN97H, J. Hazard. Mater. 102 (2003) 257–275.
[9] M. Hunsom, K. Pruksathorn, S. Damronglerd, H. Vergnes, P. Duverneuil, Electrochemical treatment of heavy metals (Cu^{2+}, Cr^{6+}, Ni^{2+}) from industrial effluent and modeling of copper reduction, Water Res. 39 (2005) 610–616.
[10] H. Shaalan, M. Sorour, S. Tewfik, Simulation and optimization of a membrane system for chromium recovery from tanning wastes, Desalination 141 (2001) 315–324.
[11] J. Rubio, M.L. Souza, R.W. Smith, Overview of flotation as a wastewater treatment technique, Miner. Eng. 15 (2002) 139–155.
[12] Y.J. Liang, L.Y. Chai, X.B. Min, C.J. Tang, H.J. Zhang, Y. Ke, X.D. Xie, Hydrothermal sulfidation and floatation treatment of heavy-metal-containing sludge for recovery and stabilization, J. Hazard. Mater. 217–218 (2012) 307–314.
[13] D. Mohan, K.P. Singh, Single- and multi-component adsorption of cadmium and zinc using activated carbon derived from *bagasse*—An agricultural waste, Water Res. 36 (2002) 2304–2318.
[14] M. Kobya, E. Demirbas, E. Senturk, M. Ince, Adsorption of heavy metal ions from aqueous solutions by activated carbon prepared from apricot stone, Bioresour. Technol. 96 (2005) 1518–1521.
[15] T.A. Kurniawan, G.Y.S. Chan, W.H. Lo, S. Babel, Physico–chemical treatment techniques for wastewater laden with heavy metals, Chem. Eng. J. 118 (2006) 83–98.
[16] Y.H. Chen, Y.D. Chen, Kinetic study of Cu(II) adsorption on nanosized $BaTiO_3$ and $SrTiO_3$ photocatalysts, J. Hazard. Mater. 185 (2011) 168–173.
[17] F. Fu, Q. Wang, Removal of heavy metal ions from wastewaters: A review, J. Environ. Manage. 92 (2011) 407–418.
[18] D.H. Park, S.R. Lim, Y.S. Yun, J.M. Park, Reliable evidences that the removal mechanism of hexavalent chromium by natural biomaterials is adsorption-coupled reduction, Chemosphere 70 (2007) 298–305.
[19] H. Bag, M. Lale, A.R. Turker, Determination of iron and nickel by flame atomic absorption spectrophotometry after preconcentration on *Saccharomyces cerevisiae* immobilized sepiolite, Talanta 47 (1998) 689–696.
[20] M.A. Shaker, H.M. Albishri, Dynamics and thermodynamics of toxic metals adsorption onto soil-extracted humic acid, Chemosphere 111 (2014) 587–595.
[21] M.A. Shaker, Thermodynamic profile of some heavy metal ions adsorption onto biomaterial surfaces, Am. J. Appl. Sci. 4 (2007) 605–612.
[22] E.A. Ghabbour, M. Shaker, A. El-Toukhy, I.M. Abid, G. Davies, Thermodynamics of metal cation binding by a solid soil derived humic acid. 2. Binding of Mn(II), and Hg(II), Chemosphere 64 (2006) 826–833.
[23] M.A. Shaker, H.M. Hussein, Heavy-metal adsorption by non-living biomass, Chem. Ecol. 21 (2005) 303–311.
[24] H.M. Huessien, A.E. Ali, M.A. Shaker, Continuous combined biological–chemical treatment of tannery wastewater, Bull. Chem. Technol. Macedonia 26 (2007) 153–158.
[25] H.M. Huessien, M.A. Shaker, A.E. Ali, Site occupation in the biosorption of some heavy metal ions by non-living *Pseudomonas* spp., New Egypt. J. Microbiol. 7 (2004) 151–160.
[26] M.E. Mahmoud, A.A. Yakout, H. Abdel-Aal, M.M. Osman, Immobilization of *Fusarium verticillioides* fungus on nano-silica (NSi–Fus): A novel and efficient biosorbent for water treatment and solid phase extraction of Mg(II) and Ca(II), Bioresour. Technol. 134 (2013) 324–330.
[27] M.E. Mahmoud, A.A. Yakout, H. Abdel-Aal, M.M. Osman, High performance SiO_2-nanoparticles-immobilized-*Penicillium funiculosum* for bioaccumulation and solid phase extraction of lead, Bioresour. Technol. 106 (2012) 125–132.
[28] M.E. Mahmoud, A.A. Yakout, M.M. Osman, Dowex anion exchanger-loaded-baker's yeast as bi-functionalized biosorbents for selective extraction of anionic and cationic mercury(II) species, J. Hazard. Mater. 164 (2012) 1036–1044.
[29] M.E. Mahmoud, A.A. Yakout, S.B. Ahmed, M.M. Osman, Speciation, selective extraction and preconcentration of chromium ions via alumina-functionalized-isatin-thiosemicarbazone, J. Hazard. Mater. 158 (2008) 541–548.
[30] M.E. Mahmoud, A.A. Yakout, H. Abdel-Aal, M.M. Osman, Enhanced biosorptive removal of cadmium from aqueous solutions by silicon dioxide nano-powder, heat inactivated and immobilized *Aspergillus ustus*, Desalination 279 (2011) 291–297.
[31] S. Ricordel, S. Taha, I. Cisse, G. Dorange, Heavy metals removal by adsorption onto peanut husks carbon: Characterization, kinetic study and modeling, Sep. Purif. Technol. 24 (2001) 389–401.
[32] R. Gnanasambandam, A. Proctor, Determination of pectin degree of esterification by diffuse reflectance fourier transform infrared spectroscopy, Food Chem. 68 (2000) 327–332.
[33] M. Iqbal, A. Saeed, S.I. Zafar, Hybrid biosorbent: An innovative matrix to enhance the biosorption of Cd(II) from aqueous solution, J. Hazard Mater. 148 (2007) 47–55.
[34] F.T. Li, H. Yang, Y. Zhao, R. Xu, Novel modified pectin for heavy metal adsorption, Chin. Chem. Lett. 18 (2007) 6017–6027.

[35] M. Jain, V.K. Garg, K. Kadirvelu, Chromium(VI) removal from aqueous system using *Helianthus annuus* (sunflower) stem waste, J. Hazard. Mater. 162 (2009) 365–372.
[36] N.V. Farinella, G.D. Matos, M.A.Z. Arruda, Grape bagasse as a potential biosorbent of metals in effluent treatments, Bioresour. Technol. 98 (2007) 1940–1946.
[37] G. Guibaud, N. Tixier, Relation between extracellular polymers' composition and its ability to complex Cd, Cu and Pb, Chemosphere 52 (2003) 1701–1710.
[38] X. Li, Y. Tang, X. Cao, D. Lu, F. Luo, W. Shao, Preparation and evaluation of orange peel cellulose adsorbents for effective removal of cadmium, zinc, cobalt and nickel, Colloid Surf. A 317 (2008) 512–521.
[39] U. Garg, M.P. Kaur, G.K. Jawa, D. Sud, V.K. Garg, Removal of cadmium(II) from aqueous solutions by adsorption on agricultural waste biomass, J. Hazard. Mater. 154 (2008) 1149–1157.
[40] R. Ashkenazy, L. Gottlieb, S. Yannai, Characterization of acetone-washed yeast biomass functional groups involved in lead biosorption, Biotechnol. Bioeng. 55 (1997) 1–10.
[41] K. Conrad, H.C. Bruun Hansen, Sorption of zinc and lead on coir, Technology. 98 (2007) 89–97.
[42] J.L. Wang, Biosorption of copper(II) by chemically modified biomass of *Saccharomyces cerevisiae*, Process Biochem. 37 (2002) 847–850.
[43] M.E. Mahmoud, I.M.M. Kenawy, M.M. Hafez, R.R. Lashein, Removal, preconcentration and determination of trace heavy metal ions in water samples by AAS via chemically modified silica gel N-(1-carboxy-6-hydroxy) benzylidenepropylamine ion exchanger, Desalination 250 (2010) 62–70.
[44] M.E. Mahmoud, M.M. Osman, O.F. Hafez, A.H. Hegazi, E. Elmelegy, Removal and preconcentration of lead(II) and other heavy metals from water by alumina adsorbents developed by surface-adsorbed-dithizone, Desalination 251 (2010) 123–130.
[45] B.E. Reed, S. Arunachalam, Use of granular activated carbon columns for lead removal, Environ. Eng. 120 (1994) 416–436.
[46] A. Kapoor, T. Viraraghavan, D.R. Cullimore, Removal of heavy metals using the fungus *Aspergillus niger*, Technology 70 (1999) 95–104.
[47] H. Freundlich, Über die adsorption in lösungen (Over the adsorption in solution), Z. Phys. Chem. 57 (1906) 385–470.
[48] I. Langmuir, The constitution and fundamental properties of solids and liquids. Part I. solids, J. Am. Chem. Soc. 38 (1916) 2221–2295.
[49] T.N. Weber, R.K. Chakravorti, Pore and solid diffusion models for fixed bed adsorbers, AlChE J. 20 (1974) 228–238.
[50] D.O. Hayward, B.M.W. Trapnell (Eds.), Chemisorption, second edition, Butterworths, London, 1964.
[51] S.J. Thomson, G. Webb, Heterogeneous Catalysis, Oliver and Boyd, Edinburgh, 1968.
[52] M.M. Dubinin, L.V. Radushkevich, Lead removal from aqueous solution by natural and pretreated clinoptilolite: Adsorption equilibrium and kinetics, Proc. Acad. Sci. USSR Phys. Chem. Sect. 55 (1947) 331.
[53] A. Günay, E. Arslankaya, İsmail Tosun, Lead removal from aqueous solution by natural and pretreated clinoptilolite: Adsorption equilibrium and kinetics, J. Hazard. Mater. 146 (2007) 362–371.
[54] A. Dąbrowski, Adsorption—from theory to practice, Adv. Colloid Interface Sci. 93 (2001) 135–224.
[55] O. Altın, H.O. Özbelge, T. Doğu, Use of general purpose adsorption isotherms for heavy metal–clay mineral interactions, J. Colloid Interface Sci. 198 (1998) 130–140.
[56] J.P. Hobson, Physical adsorption isotherms extending from ultrahigh vacuum to vapor pressure, J. Phys. Chem. 73 (1969) 2720–2727.
[57] K. Saltalı, A. Sarı, M. Aydın, Removal of ammonium ion from aqueous solution by natural Turkish (Yıldızeli) zeolite for environmental quality, J. Hazard. Mater. 141 (2007) 258–263.
[58] H. Zheng, D. Liu, Y. Zheng, S. Liang, Z. Liu, Sorption isotherm and kinetic modeling of aniline on Cr–bentonite, J. Hazard. Mater. 158 (2008) 65–72.
[59] A. Özcan, E.M. Öncü, A.S. Özcan, Kinetics, isotherm and thermodynamic studies of adsorption of Acid Blue 193 from aqueous solutions onto natural sepiolite, Colloid Surf. A 277 (2006) 90–97.
[60] B. Erdem, A. Özcan, Ö. Gök, A.S. Özcan, Immobilization of 2,2´-dipyridyl onto bentonite and its adsorption behavior of copper(II) ions, J. Hazard. Mater. 163 (2009) 418–426.
[61] Y.S. Ho, Citiation review of Lagergren kinetic rate equation on adsorption reactions, Scientometrics 59 (2004) 171–177.
[62] Y.S. Ho, G. McKay, Pseudo-second order model for sorption processes, Process Biochem. 34 (1999) 451–465.
[63] S.H. Chien, W.R. Clayton, Application of Elovich equation to the kinetics of phosphate release and sorption in soils, Soil Sci. Soc. Am. J. 44 (1980) 265–268.
[64] S.K. Srivastava, R. Tyagi, N. Pant, Adsorption of heavy-metal ions on carbonaceous material developed from the waste slurry generated in local fertilizer plants, Water Res. 23 (1989) 1161–1165.
[65] Y.F. Lin, H.W. Chen, P.S. Chien, C.S. Chiou, C.C. Liu, Application of bifunctional magnetic adsorbent to adsorb metal cations and anionic dyes in aqueous solution, J. Hazard. Mater. 185 (2011) 1124–1130.
[66] R.R. Sheha, A.A. El-Zahhar, Synthesis of some ferromagnetic composite resins and their metal removal characteristics in aqueous solutions, J. Hazard. Mater. 150 (2008) 795–803.
[67] Y. Wang, H. Gao, J. Sun, J. Li, Y. Su, Y. Ji, C. Gong, Selective reinforced competitive biosorption of Ag(I) and Cu(II) on *Magnetospirillum gryphiswaldense*, Desalination 270 (2011) 258–263.
[68] A. Saeed, M. Iqbal, Bioremoval of cadmium from aqueous solution by black gram husk (*Cicer arientinum*), Water Res. 37 (2003) 3472–3480.